JPn Neuroscience
The Journal of Physiology

Evolutionarily conserved differences in pallial and thalamic short-term synaptic plasticity in striatum

Jesper Ericsson, Marcus Stephenson-Jones, Andreas Kardamakis, Brita Robertson, Gilad Silberberg and Sten Grillner

Nobel Institute for Neurophysiology, Department of Neuroscience, Karolinska Institutet, SE-171 77 Stockholm, Sweden

Key points

- Recent studies have shown that the striatum and the basal ganglia are to a remarkable degree conserved throughout the vertebrate phylum.
- As the basic organization of the neural machinery for action selection is present in the lamprey, it is essential to understand how the striatum is activated.
- In this study we characterize the pharmacology and synaptic dynamics from the lateral pallium (LPal; cortex) and thalamus (Th), the main excitatory input to the striatum.
- We show that, as in mammals, the LPal and Th provide glutamatergic excitation to the striatum, but with completely opposite short-term synaptic plasticity due to differences in presynaptic properties.
- These synaptic differences are also characteristic of the mammalian striatum, suggesting that these are fundamental components of the vertebrate mechanisms for action selection.

Abstract The striatum of the basal ganglia is conserved throughout the vertebrate phylum. Tracing studies in lamprey have shown that its afferent inputs are organized in a manner similar to that of mammals. The main inputs arise from the thalamus (Th) and lateral pallium (LPal; the homologue of cortex) that represents the two principal excitatory glutamatergic inputs in mammals. The aim here was to characterize the pharmacology and synaptic dynamics of afferent fibres from the LPal and Th onto identified striatal neurons to understand the processing taking place in the lamprey striatum. We used whole-cell current-clamp recordings in acute slices of striatum with preserved fibres from the Th and LPal, as well as tract tracing and immunohistochemistry. We show that the Th and LPal produce monosynaptic excitatory glutamatergic input through NMDA and AMPA receptors. The synaptic input from the LPal displayed short-term facilitation, unlike the Th input that instead displayed strong short-term synaptic depression. There was also an activity-dependent recruitment of intrastriatal oligosynaptic inhibition from both inputs. These results indicate that the two principal inputs undergo different activity-dependent short-term synaptic plasticity in the lamprey striatum. The difference observed between Th and LPal (cortical) input is also observed in mammals, suggesting a conserved trait throughout vertebrate evolution.

(Received 17 May 2012; accepted after revision 1 November 2012; first published online 12 November 2012)
Corresponding author S. Grillner: Nobel Institute for Neurophysiology, Department of Neuroscience, Karolinska Institutet, SE-171 77 Stockholm, Sweden. Email: sten.grillner@ki.se

Abbreviations aCSF, artificial cerebrospinal fluid; AP-5, D-(−)-2-amino-5-phosphonopentanoic acid; IRN, Inwardly Rectifying Neuron; Kir, inwardly rectifying potassium channels; LPal, lateral pallium; MSNs, medium spiny neurons; NBQX, 2,3-dioxo-6-nitro-1,2,3,4-tetrahydrobenzo[*f*]quinoxaline-7-sulphonamide; PB, phosphate buffer; PPD, paired-pulse depression; PPF, paired-pulse facilitation; PPR, paired-pulse response; PSP, postsynaptic potential; RTR, recovery test response; Th, thalamus; vLPal, ventrolateral pallium.

DOI: 10.1113/jphysiol.2012.236869

Introduction

The input layer of the basal ganglia, the striatum, receives abundant cortical and thalamic (Th) input, and serves a critical role in the integration and processing of motor-related signalling and cognitive behaviour (Graybiel, 2005; Grillner *et al.* 2005). In the lamprey, one of the earliest vertebrates that diverged from the main vertebrate evolutionary line some 560 million years ago (Kumar & Hedges, 1998), the largest striatal input also arises from the lateral pallium (LPal; the homologue of the cortex) and the Th (Polenova & Vesselkin, 1993; Northcutt & Wicht, 1997; Pombal *et al.* 1997*b*), which are in focus here. It also receives a dopaminergic, 5-HT and histaminergic input (Brodin *et al.* 1990*a*,*b*; Jimenez *et al.* 1996; Pombal *et al.* 1997*b*).

The organization of the basal ganglia is to a remarkable degree conserved throughout the vertebrate phylum (Marín *et al.* 1998; Reiner *et al.* 1998; Smeets *et al.* 2000; Stephenson-Jones *et al.* 2011). Recent studies have shown that all the principal components of the basal ganglia (the striatum, globus pallidus externa and interna, subthalamic nucleus and substantia nigra pars reticulata/compacta) are present in lamprey (Pombal *et al.* 1997*a*,*b*; Robertson *et al.* 2006, 2007; Ericsson *et al.* 2011; Stephenson-Jones *et al.* 2011, 2012). Moreover, the molecular characteristics of the striatum are similarly conserved like the expression of GABA, substance P and enkephalin, and dopamine D1 and D2 receptors (Pombal *et al.* 1997*a*; Robertson *et al.* 2007, 2012; Ericsson *et al.* 2011; Stephenson-Jones *et al.* 2011). In the striatum, two main types of neurons have been described: GABAergic inwardly rectifying neurons (IRNs) expressing potassium channels of the Kir type; and non-inwardly rectifying neurons including fast-spiking neurons (Ericsson *et al.* 2011). The former are of two subtypes expressing substance P or enkephalin, respectively. They are similar to the mammalian, avian and reptile spiny projection neurons (Kawaguchi *et al.* 1989; Farries & Perkel, 2000; Farries *et al.* 2005; Barral *et al.* 2010), and project to the lamprey homologues of the globus pallidus and substantia nigra pars reticulata (Stephenson-Jones *et al.* 2011, 2012).

The afferent synaptic input to the striatum of lamprey has so far not been studied. The aim here is to characterize the synaptic effects from the LPal and Th, representing the main afferents to the striatum. In rodents, the corticostriatal and thalamostriatal synapses onto medium spiny neurons (MSNs) are glutamatergic, but they have distinct properties (Smith *et al.* 2001; Smeal *et al.* 2007; Ding *et al.* 2008, 2010). Activation of corticostriatal fibres leads to short-term synaptic facilitation, in contrast to thalamostriatal synapses that exhibit short-term synaptic depression. We find the same difference in synaptic properties in lamprey between the two inputs as established in mammals, suggesting the difference in activity-dependent short-term plasticity is conserved throughout vertebrate evolution.

Methods

Ethical approval

All experimental procedures were approved by the local ethical committee (Stockholm's Norra Djurförsöksetiska Nämnd), and were in accordance with The Guide for the Care and Use of Laboratory Animals (National Institutes of Health, 1996 revision). During the investigation, every effort was made to minimize animal suffering and to reduce the number of animals used. Experiments were performed on a total of 79 adult river lampreys (*Lampetra fluviatilis*).

Slice preparation

The dissection and removal of brains from deeply anaesthetized (MS-222; 100 mg l^{-1}; Sigma, St Louis, MO, USA) animals were performed as described in detail previously (Ericsson *et al.* 2007). To facilitate the cutting of brain slices on a microtome (Microm HM 650V; Thermo Scientific, Walldorf, Germany), pre-heated liquid agar (Sigma) dissolved in water at a concentration of 4% was prepared. The agar was allowed to cool down for a few minutes before brains were embedded in the agar, on top of a metal plate placed on ice. This ensured that the agar directly solidified around the brain and that the agar was cooled down quickly to restrict it from warming the brain tissue. The agar block containing the brain was then glued to a metal plate and transferred to ice-cold artificial cerebrospinal fluid (aCSF) with the following composition (in mM): NaCl, 125; KCl, 2.5; $MgCl_2$, 1; NaH_2PO_4, 1.25; $CaCl_2$, 2; $NaHCO_3$, 25; glucose, 8. The aCSF was oxygenated continuously with 95% O_2 and 5% CO_2 (pH 7.4). Transverse brain slices of 350–400 μm were cut at the level of the striatum (Fig. 1) and allowed to recover at ~5°C for at least 1 h before being transferred to a submerged recording chamber. Perfusion of the slices was performed with aCSF at 6–8°C (Peltier cooling system; ELFA, Solna, Sweden). In a few experiments an alternative Mg^{2+}-free solution was used to remove the voltage-gated Mg^{2+} block of NMDA receptors to increase the likelihood of activating these receptors. The composition of this solution was the same as the regular aCSF apart from the complete removal of $MgCl_2$. Neurons were visualized with DIC/infrared optics (Olympus BX51WI, Tokyo, Japan).

Electrophysiology

Whole-cell current-clamp recordings were performed with patch pipettes made from borosilicate glass

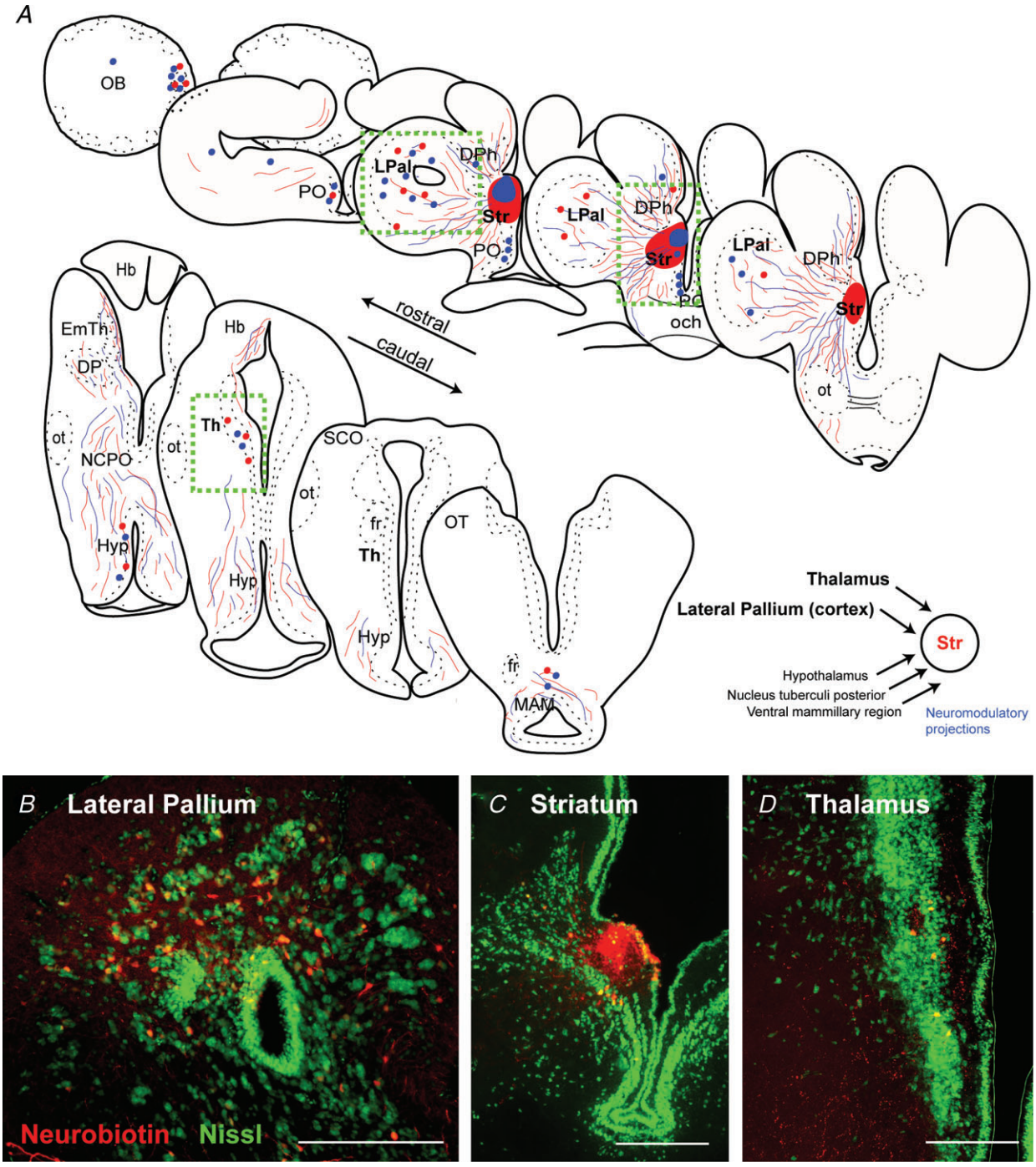

Figure 1. Mapping of striatal afferent input
A, schematic transverse sections through the lamprey brain showing the location of retrogradely labelled cells (red and blue dots) and anterogradely labelled fibres (red and blue lines) from two injection sites (neurobiotin) into the striatum. Injection site in the striatum (*C*) resulted in retrogradely labelled neurons throughout the LPal (*B*) and the Th (*D*). In addition, retrograde labelled neurons were observed in the olfactory bulbs, preoptic nucleus, medial pallium, hypothalamus, nucleus tuberculi posterior and mammillary area. Nissl stain in green in *B–D*. Scale bars, 200 μm in *B–D*. DPh, habenula projecting dorsal pallidum; EmTh, eminentia thalami; fr, fasciculus retroflexus; Hb, habenula; Hyp, hypothalamus; LPal, lateral pallium; MAM, mammillary area; NCPO, nucleus of the postoptic commissure; OB, olfactory bulb; och, optic chiasm; ot, optic tract; OT, optic tectum; PO, preoptic nucleus; SCO, subcommissural organ; Str, striatum; Th, thalamus.

microcapillaries (Harvard Apparatus, Kent, UK) using a horizontal puller (Model P-97; Sutter Instruments, Novato, CA, USA). The resistance of recording pipettes were typically 7–12 MΩ when filled with intracellular solution of the following composition (in mM): potassium gluconate, 131; KCl, 4; phosphocreatine disodium salt, 10; Hepes, 10; Mg-ATP, 4; Na-GTP, 0.3 (osmolarity 265–275 mosmol l^{-1}). To facilitate the detection of GABA currents at resting potential, an alternative intracellular solution with a higher chloride concentration was used in a few experiments in order to shift the reversal potential for GABA to more depolarized values. The composition of this solution was as follows (in mM): potassium gluconate, 105; KCl, 30; phosphocreatine disodium salt, 10; Hepes, 10; Mg-ATP, 4; Na-GTP, 0.3. The calculated reversal potential for GABA for the two solutions was −85 mV (low intracellular Cl^- concentration) and −35 mV (intermediate intracellular Cl^-). Bridge balance and pipette capacitance compensation were adjusted for on the Axoclamp 2B amplifier (Molecular Devices Corp., CA, USA), and all membrane potential values were corrected for the liquid junction potential (∼10 mV). Data collection and analysis were made with ITC-18 (HEKA, Lambrecht, Germany) and Igor software (version 6.03; WaveMetrics, Portland, OR, USA). At least 20 individual responses were averaged from each stimulation locus of presynaptic fibres.

A total of 69 cells were included in the study based partly on the inclusion criteria that their resting membrane potentials were below −50 mV and had action potentials reaching above 0 mV. Extracellular stimulation of usually 100 μs duration (range 50–300 μs) of striatal afferents was performed with a concentric bipolar metal electrode (FHC, Bowdoin, ME, USA) connected to a constant current isolated stimulator (Digitimer, Hertfordshire, UK). The stimulation intensity was set to about one–two times the threshold strength (typically 100–200 μA) to evoke postsynaptic potentials (PSPs). At this intensity, minor changes ($\leq$10 μm) of the location of the stimulation electrode resulted in profound differences in response amplitudes and dynamics, indicating low current spread from the stimulation. To investigate the short-term dynamics of synaptic transmission, a stimulus train of eight pulses at 10 Hz was used together with a recovery test pulse 600 ms after the 8th pulse (see Planert *et al.* 2010). We initially also tested other frequencies (20 Hz, 40 Hz and 70 Hz), but as all experiments were performed at lamprey physiological temperatures (5–10°C), the slow time constants made it difficult to assess individual postsynaptic responses within the pulse train at these frequencies. Also, at 10 Hz stimulation frequency, significant short-term synaptic plasticity has been shown in mammals (Ding *et al.* 2008). PSPs often started on the decay phase of previous responses, and to extract correct amplitudes the synaptic decay was either fitted by an exponential curve and subtracted or manually subtracted (see Planert *et al.* 2010). The paired-pulse ratio was calculated by dividing the second PSP by the first PSP in a response train, and the recovery test response (RTR) ratio by comparing the 9th PSP with the first PSP.

Before stimulation experiments were performed, the exact location of afferent fibre bundles from the LPal, Th and olfactory bulbs within the same transverse plane as the striatum were mapped out by neurobiotin injections to anterogradely label fibres. Pharmacological agents were bath-applied through the perfusion system. Glutamate AMPA receptors were blocked by 2,3-dioxo-6-nitro-1,2,3,4-tetrahydrobenzo[*f*]quinoxaline-7-sulphonamide (NBQX; 40 μM; Tocris, Ellisville, MO, USA), and NMDA receptors with D-(−)-2-amino-5-phosphonopentanoic acid (AP-5; 50 μM; Tocris). The NMDA/AMPA ratio was calculated by comparing the area under the first two responses (before GABAergic signals were recruited), where the NMDA component was calculated by subtracting the non-AP-5 sensitive area (AMPA) from the control area. $GABA_A$ receptors were blocked by gabazine (20 μM; Tocris). To investigate the dynamic properties of activated GABA fibres, responses were measured after application of NBQX/AP-5 and before additional application of gabazine that completely removed responses. Experiments assessing differences in short-term synaptic plasticity by altering extracellular calcium concentrations were performed in the presence of AP-5.

Anatomy

The animals were deeply anaesthetized in tricaine methane sulphonate (MS-222; 100 mg l^{-1}; Sigma) diluted in fresh water. They were then transected caudally at the seventh gill, and the dorsal skin and cartilage were removed to expose the brain. During the dissection and the injections, the head was pinned down and submerged in ice-cooled oxygenated Hepes-buffered physiological solution (in mM: NaCl, 138; KCl, 2.1; $CaCl_2$, 1.8; $MgCl_2$, 1.2; glucose, 4; Hepes, 2), pH 7.4.

Retrograde tracing

All injections were made with glass (borosilicate, OD = 1.5 mm, ID = 1.17 mm) micropipettes, with a tip diameter of 10–20 μm. The micropipettes were mounted in a holder, which was attached to an air supply to enable pressure-injection of dyes, and the pipette was mounted on a Narishige micromanipulator.

Tracing experiments

Neurobiotin (50–200 nl, 20%; Vector, Burlingame, CA, USA; in distilled water containing fast green to aid

visualization of the spread of the injection) was pressure-injected unilaterally into: (i) the striatum ($n = 9$); (ii) the Th ($n = 3$); and (iii) the LPal ($n = 4$).

Dissection and histology

Following injections, the heads were kept submerged in aCSF in the dark at 4°C for 24 h to allow retrograde transport of the tracers. The brains were then dissected out of the surrounding tissue and fixed by immersion in 4% formalin and 14% saturated picric acid in 0.1 M phosphate buffer (PB) pH 7.4 for 12–24 h, after which they were cryoprotected in 20% sucrose in PB for 3–12 h. Transverse 20-μm-thick sections were made using a cryostat, collected on gelatine-coated slides and stored at −20°C until further processing. For GABA and glutamate immunohistochemistry, tissue was fixed by immersion in 4% formalin, 1% glutaraldehyde and 14% of a saturated solution of picric acid in 0.1 M PB. The brain was postfixed for 24–48 h and cryoprotected as described above.

Immunohistochemistry

For the immunohistochemical detection of GABA and glutamate, the brains were injected, dissected and processed as described above. Sections were then incubated overnight with either a mouse monoclonal anti-GABA antibody (1:1000, mAb, 3A12, kindly donated by Dr Peter Streit, Zurich, Switzerland; Matute & Streit, 1986; Robertson *et al.* 2007) or with polyclonal rabbit anti-glutamate antibody (1:500; AB133; Millipore, MA, USA). Sections were subsequently incubated with either Cy3-conjugated donkey anti-mouse IgG (GABA) or Cy3-conjugated donkey anti-rabbit IgG (glutamate), together with Cy2-conjugated streptavidin (1:1000; Jackson Immunoresearch, Suffolk, United Kingdom) for 2 h and coverslipped.

Statistics

Results are presented as mean ± SEM, and statistical comparisons between means were made with two-tailed paired *t* tests with GraphPad Prism Software (GraphPad Software, San Diego, CA, USA) or Microsoft Excel (Microsoft, Seattle, WA, USA). In figures, one star indicates $P < 0.05$, two stars $P < 0.01$ and three stars $P < 0.001$.

Results

Afferent input from the LPal and Th to the striatum

In order to identify the location of the LPal and Th cells projecting to the striatum, neurobiotin was injected into the striatum to retrogradely label afferent cell bodies (Fig. 1*A* and *C*; $n = 5$). Retrogradely labelled cells were observed unilaterally throughout the entire rostrocaudal extent of the LPal, with the highest density of cells in the dorsal two-thirds of the LPal and only a few labelled cells in the ventral part of the LPal (Fig. 1*A* and *B*). Dorsal to the striatum a few cells were also observed in the medial pallium (Fig. 1*A*). Further caudally, retrogradely labelled cells were observed in the Th (Fig. 1*A* and *D*), as previously reported (Pombal *et al.* 1997*b*).

In agreement with published data, a few retrogradely labelled neurons were also observed in the lateral olfactory bulbs, and a cluster of neurons was retrogradely labelled in the medial olfactory bulbs (Fig. 1*A*). Anterograde tracing studies have confirmed that this latter population projects directly to the nucleus tuberculi posterior (Derjean *et al.* 2010) and may not terminate in the striatum, allowing for the possibility that this population of neurons may have been labelled through uptake from fibres of passage. In addition, retrogradely labelled cells were observed in the region of the hypothalamus, in the dopaminergic nucleus tuberculi posterior, and a few cells were observed in the adjacent mammillary region (Fig. 1*A*).

To determine the location and projection patterns of the thalamostriatal and palliostriatal fibre tracts within the transverse brain slice used (see Methods), we injected neurobiotin into the Th and LPal, respectively. Injections in the Th anterogradely labelled fibres that approached the striatum through a dense fibre tract projecting via the most lateral portion of the medial pallium (Fig. 2*A*), confirming the previously described Th projection in lamprey (Polenova & Vesselkin, 1993; Pombal *et al.* 1997*b*). These thalamostriatal axons innervate the dorsal part of the striatum where many striatal dendrites are located (Ericsson *et al.* 2011), and are also observed ventral to the striatal cell band (Fig. 2*B*). Fibres of a second, ventral thalamo-telencephalic projection (Northcutt & Wicht, 1997) were rarely seen. Injections in the LPal anterogradely labelled two fibre bundles, one that projected ventrally towards the striatum (Fig. 2*C*) where small varicose fibres terminate throughout the lateral and ventral striatal neuropil (Northcutt & Wicht, 1997). The second projected dorsally through the medial pallium and has been shown to project through the habenula commissure to the contralateral LPal (Northcutt & Wicht, 1997). The anterogradely labelled fibres from the LPal were observed throughout the striatum both dorsal and ventral of the striatal cell band (Fig. 2*D*). In contrast to the labelling from the Th injections, fibres were also observed through the dense striatal cell band. The results thus showed that the afferent fibres from the LPal and Th project to the striatum through topographically separate fibre bundles, indicating that their synaptic contacts onto striatal cells may be investigated separately.

A transverse striatal slice maintains lateral palliostriatal and thalamostriatal axons

To study the physiological responses in the striatum to stimulation of LPal and Th afferents in an acute transverse brain slice preparation (350–400 μm thickness; see Methods), we first investigated the responsiveness of striatal neurons to stimulations of different areas within the slice (Fig. 3*A*) to confirm that afferent fibres were preserved. A stimulus train readily evoked striatal PSPs when applied to the Th fibres (Fig. 3*Aa*, Th input indicated in both hemispheres by dark grey shading), to the area dorsal to the striatum (Fig. 3*Ab*) and in the LPal (Fig. 3*Ac* and *d*), as well as to the most ventral part of LPal (vLPal; Fig. 3*Ae*). The light grey shading in Fig. 3*A* indicates areas where striatal responses were easily evoked, including the red shading indicating the stimulation area of LPal. No responses were evoked from the very lateral part of LPal (border region of the grey shading and in the unshaded area) unless significantly higher stimulation strength was used (>4× the threshold stimulus strength in LPal).

Activation of the Th fibre bundles ($n = 17$; Fig. 3*Aa*) elicited PSPs that reached a plateau after the second or third response, as did responses to the adjacent area located inbetween the Th fibre bundle and the striatum ($n = 8$; Fig. 3*Ab*). In contrast, responses from LPal ($n = 17$; Fig. 3*Ac* and *d*) in all cases summated effectively over several responses, while stimulation of vLPal ($n = 10$; Fig. 3*Ae*) displayed a similar behaviour to that of the Th input. Responses were recorded from the two main cell types that have been classified in the lamprey striatum, inwardly rectifying neurons (Fig. 3*B*) resembling mammalian MSNs and those with little or no rectification (Fig. 3*C*; Ericsson *et al.* 2011). There was no difference between the postsynaptic responses of rectifying neurons ($n = 30$) and non-rectifying neurons ($n = 32$, not illustrated).

The results thus show that the fibres from the LPal and Th onto striatal neurons are preserved in the same slice and innervate both types of neurons. Below we will report on the type of synaptic transmission from the LPal and Th, and their differences in activity-dependent short-term plasticity onto striatal neurons.

Input from the LPal is glutamatergic and drives intrastriatal GABAergic oligosynaptic inhibition

In mammals the main excitatory synaptic drive to the striatum is glutamatergic, and it was important to confirm that this is the case also in lamprey. We therefore investigated the connections from the LPal in greater detail and if glutamatergic antagonists could affect the synaptic transmission. Stimulation of the LPal (Fig. 4*A*) evoked synaptic responses (Fig. 4*B*, black trace) that were completely suppressed by application of AP-5 (50 μM) and NBQX (40 μM; Fig. 4*B*, blue trace). This was quantified by comparing the amplitude of the first PSP before and after drug application (control$_{PSP1}$ 2.22 ± 0.55 mV, NBQX/AP-5$_{PSP1}$

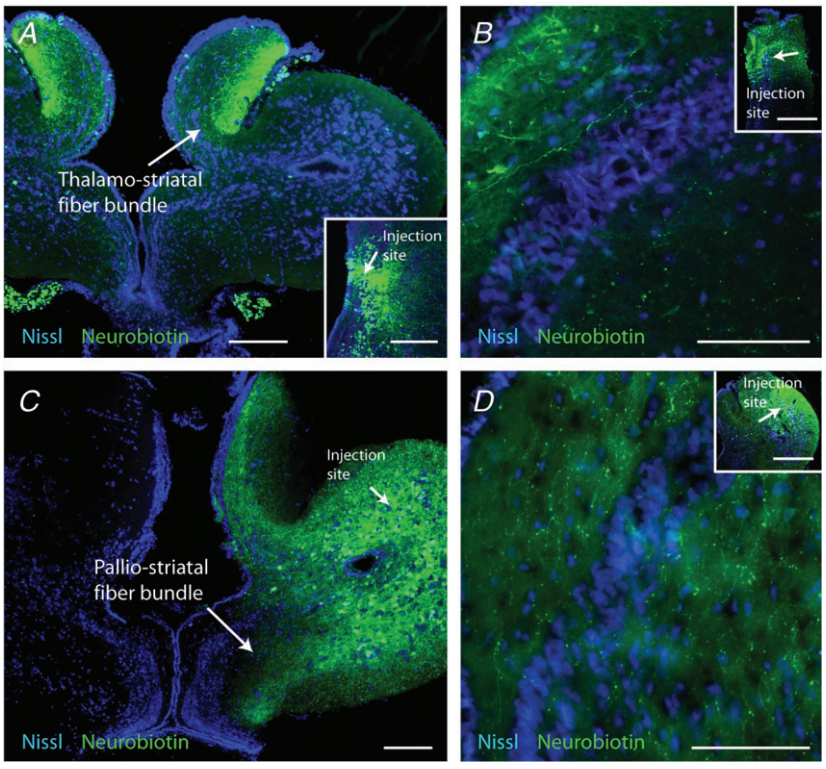

Figure 2. Mapping of lateral palliostriatal and thalamostriatal fibres
A, anterograde labelling of thalamostriatal fibres after injection of neurobiotin in the Th, injection site inserted in the bottom-right part. The dense, anterogradely labelled thalamostriatal fibre tract was located in the most lateral neuropil of the medial pallium and limited to a well-defined narrow portion of the slice towards the striatum. *B*, anterogradely labelled thalamostriatal fibres in the striatum following an injection in the Th (inset). *C*, neurobiotin injections in the LPal anterogradely labelled fibres throughout the lateral and ventral striatal neuropil (arrows). Injection site indicated in the LPal. *D*, anterogradely labelled palliostriatal fibres in the striatum following an injection in the LPal (inset). Scale bars, 200 μm in *A* and *C*; 100 μm in *B* and *D*; and 500 μm in *B* and *D* inset.

0.027 ± 0.03 mV, $P < 0.001$, $n = 6$; Fig. 4*C*). To investigate whether NMDA receptors contribute to the synaptic transmission, experiments were performed in Mg^{2+}-free aCSF (Fig. 4*D*). Application of the NMDA receptor antagonist AP-5 markedly reduced, but did not block, the synaptic transmission (Fig. 4*D*, grey trace). Additional application of the AMPA receptor antagonist NBQX completely removed all synaptic responses (Fig. 4*D*, blue trace), indicating that both receptor subtypes are activated at synapses from the LPal. The NMDA to AMPA ratio was calculated to 1.84 by dividing the area under the first two pulses of the NMDA and AMPA components (see Methods).

To investigate if a train of depolarizing synaptic potentials would also recruit a GABAergic input, we applied the $GABA_A$ receptor antagonist gabazine (20 μM) to the slice. The red trace in Fig. 4*E* shows that the synaptic responses were enhanced, except for the first two synaptic responses in the pulse train. In these experiments, neurons were held at −80 mV or more depolarized potentials, to ensure that GABA was hyperpolarizing (calculated reversal potential at −84 mV). To quantify the effect of gabazine, we compared the normalized area under the averaged trace before and after application of the antagonist (gabazine $133 \pm 10\%$ compared with control, $P < 0.01$, $n = 5$; Fig. 4*E* and *F*). Additional application of NBQX and AP-5 completely blocked all responses (gabazine/NBQX/AP-5 $5.2 \pm 3\%$, $P < 0.001$, $n = 5$; Fig. 4*E* and *F*). The GABAergic activation only occurred after the second or third EPSP, which would suggest an oligosynaptic nature of these responses; moreover NBQX/AP-5 always removed the entire synaptic response indicating that no GABAergic PSPs were activated directly by the stimulation. Slower synaptic responses were also seen by paired-pulse stimulation (Fig. 4*G*; stimulation artefacts included for clarity) and presumably GABAergic as they diminished around its reversal potential (data not shown), here recorded at −95 mV where GABA is depolarizing.

To further explore if pallial neurons projecting to the striatum indeed are glutamatergic, we combined retrograde labelling from striatum with immunohistochemistry. Retrogradely labelled cells within the LPal were immunoreactive for glutamate (Fig. 4*H* and *I*), and glutamate fibres were detected throughout the striatum (Fig. 4*J*). In contrast, the retrogradely labelled pallial cells were GABA-immunonegative (Fig. 4*K* and *L*). These results taken together thus show that the direct lateral palliostriatal connections are glutamatergic, and that this synaptic input activates both NMDA and AMPA receptors

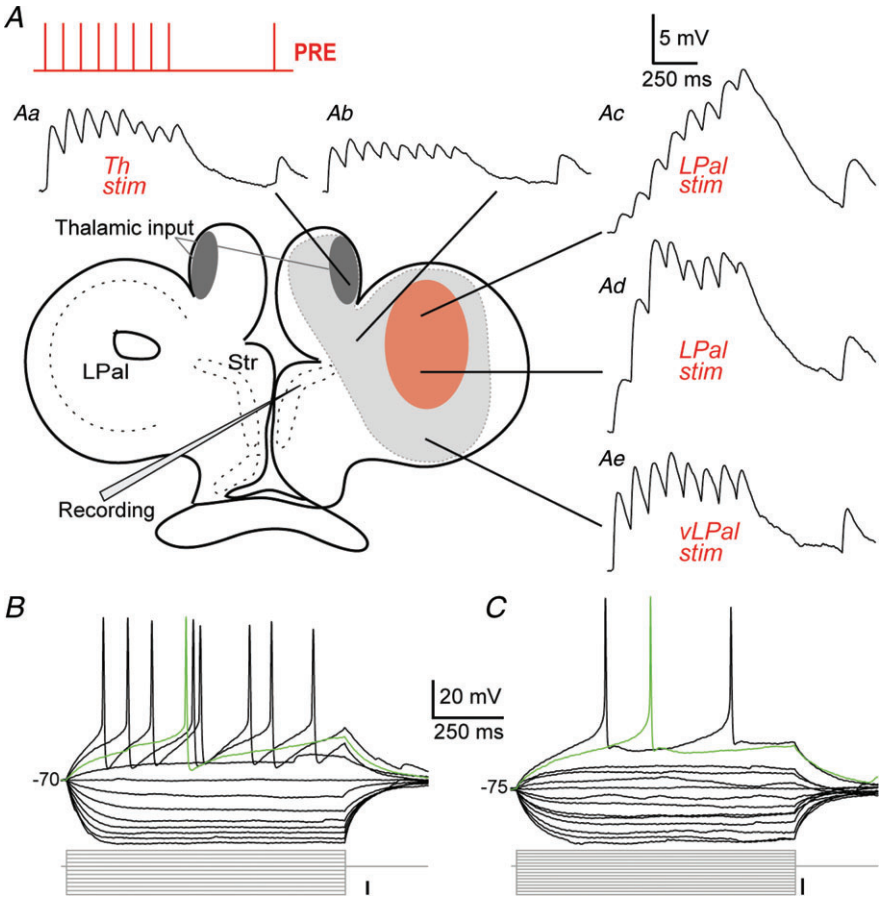

Figure 3. Extracellular stimulation of striatal afferents
A, schematic overview of a transverse brain slice indicating the extracellular stimulation sites of striatal afferents. The light grey shading indicates areas from which striatal responses were readily evoked, including a red shading of the stimulation region in the LPal. The presynaptic stimulus train of 8 + 1 pulses at 10 Hz is indicated in the top left corner. *Aa–e*, voltage responses to stimulation (stimulation artefacts removed) of Th fibres (*Aa*, thalamostriatal fibres indicated by dark grey shading), the adjacent area dorsal to the striatum (*Ab*), the LPal (*Ac* and *d*) and the most ventral part of the LPal (*Ae*). Neurons were held just below −80 mV before stimulating presynaptic fibres. *B,* recorded neurons were a mix of inwardly rectifying neurons and non-rectifying neurons (*C*), shown by their voltage responses to hyperpolarizing and depolarizing current injections. The green traces represent the first, single action potentials evoked by the depolarizing steps. Scale bars for the current injections indicate 10 pA. LPal, lateral pallium; Str, striatum; Th, thalamus; vLPal, ventrolateral pallium.

postsynaptically. Furthermore, this excitation may also recruit the intrastriatal GABAergic network as indicated by the oligosynaptic inhibitory responses.

Input from the Th is glutamatergic and drives intrastriatal GABAergic inhibition

We next investigated whether the thalamostriatal afferent input was also glutamatergic and operated through both NMDA and AMPA receptors. Extracellular stimulations were performed strictly in the area indicated in Fig. 5*A* to selectively activate Th fibres, which evoked reliable responses in 17 out of 19 recorded neurons (see example in Fig. 5*B*, black trace). Application of NBQX and AP-5 (Fig. 5*B*, blue trace) completely removed all responses ($\text{control}_{\text{PSP1}}$ 5.36 ± 0.89 mV, $\text{NBQX/AP-5}_{\text{PSP1}}$ 0.080 ± 0.033 mV, $P < 0.001$, $n = 6$; Fig. 5*C*). Experiments were also performed in Mg^{2+}-free aCSF where application of AP-5 substantially reduced the postsynaptic responses (Fig. 5*D*, grey trace), indicative of NMDA receptor activation. Additional application of NBQX (Fig. 5*D*, blue trace) completely suppressed all responses, indicative of AMPA receptor activation. The NMDA to AMPA ratio was calculated to 1.33.

As in the LPal, application of gabazine increased responses at the second pulse or later (Fig. 5*E*, red trace), quantified by comparing the normalized area under the response (gabazine $137 \pm 10\%$ compared with control, $P < 0.01$, $n = 5$; Fig. 5*F*). Additional application of NBQX and AP-5 completely blocked all responses (gabazine/NBQX/AP-5 $2.3 \pm 1\%$, $P < 0.001$, $n = 5$; Fig. 5*E* and *F*).

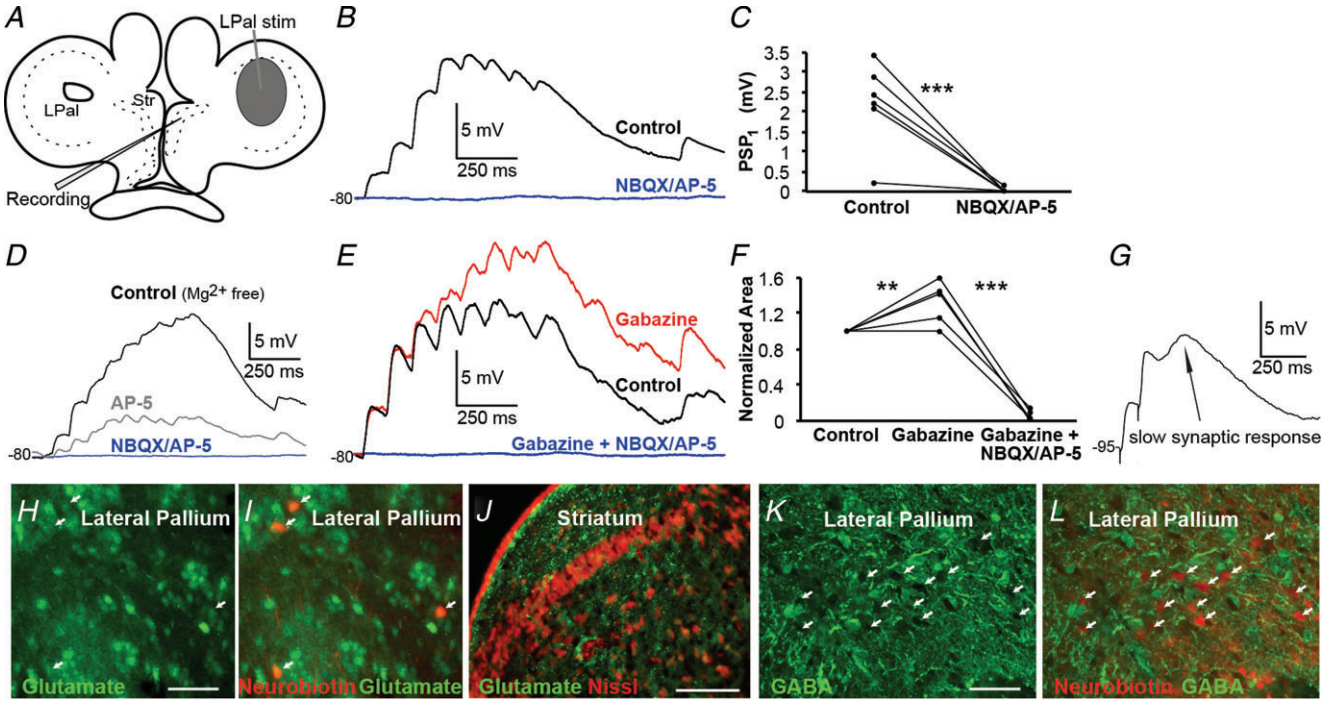

Figure 4. Lateral palliostriatal stimulation evokes glutamatergic synaptic responses
A, schematic drawing indicating the stimulation area in lateral pallium (LPal). *B*, current-clamp recordings of striatal postsynaptic potentials (PSPs) in regular aCSF evoked by LPal stimulation (artefacts removed), before (black trace) and after application of NBQX (40 μM) and AP-5 (50 μM, blue trace). *C*, application of NBQX and AP-5 completely removed the postsynaptic response, quantified by comparing the first PSP response in the train before and after drug application. *D*, NMDA and AMPA receptors were investigated in Mg^{2+}-free aCSF by current-clamp recordings of striatal PSPs evoked by LPal stimulation before (black trace) and after sequential application of AP-5 (grey trace), and both AP-5 and NBQX (blue trace) at about −80 mV. *E*, application of gabazine (20 μM, red trace) increased responses in recorded neurons (rest V_m −80 mV) indicative of oligosynaptic inhibition. Responses were completely removed by further application of NBQX and AP-5 (blue trace). *F*, quantification of the effect of drugs in (*E*) was performed by comparing the normalized area under the response curve before and after application. *G*, a slow synaptic response revealed by paired-pulse stimulation (artefacts from stimulation included for clarity). The neuron was held at a hyperpolarized potential (−95 mV) where GABA is depolarizing. *H*, immunostaining for glutamate (green) in LPal. *I*, retrogradely labelled neurons (red, indicated by arrows) in the LPal were immunostained for glutamate seen by co-staining. *J*, immunostaining showed glutamatergic fibres (green) surrounding the striatal cell band (red Nissl staining). *K*, immunostaining for GABA (green) in the LPal. *L*, retrogradely labelled neurons (red) were GABA-immunonegative as there was no co-staining with GABA. Scale bars, 50 μm in *H* and *K*; 200 μm in *J*. $^{**}P < 0.01$, $^{***}P < 0.001$, two-tailed paired *t* tests. Str, striatum.

To further corroborate that the Th neurons projecting to the striatum were glutamatergic, we combined retrograde labelling with immunohistochemistry. The retrogradely labelled cells within the Th were immunoreactive for glutamate (Fig. 4*G* and *H*), and in contrast none of the retrogradely labelled neurons was immunoreactive to GABA (Fig. 4*I* and *J*).

The results thus suggest that also the Th input is glutamatergic, and activates both NMDA and AMPA receptors, and that this excitation is able to recruit an activity-dependent oligosynaptic GABAergic synaptic response, as NBQX/AP-5 completely blocked all synaptic responses. In conclusion, the monosynaptic excitatory glutamatergic activation of the vertebrate striatum from the Th and pallium/cortex was established already in the lamprey.

Lateral palliostriatal and thalamostriatal synapses differ in their synaptic dynamics

We next investigated the short-term activity-dependent synaptic plasticity of the transmission from the LPal and Th. Responses of the 10 Hz stimulation train of $8 + 1$ pulses were normalized to the first PSP in the pulse train (Fig. 6*A*). The paired-pulse ratio of the second synaptic response to the first response (Fig. 6*A* and *B*, red trace/box) showed that the responses from LPal displayed clear paired-pulse facilitation (PPF: 1.38 ± 0.10). In contrast, responses from the Th and vLPal showed paired-pulse depression (Th PPD 0.56 ± 0.07; vLPal PPD 0.61 ± 0.12; $P < 0.001$ compared with LPal; Fig. 6*A* and *B*). Synaptic responses from the LPal were significantly facilitating for the first 300 ms after the first PSP (Fig. 6*A*; $n = 17$, red trace), unlike Th synaptic responses

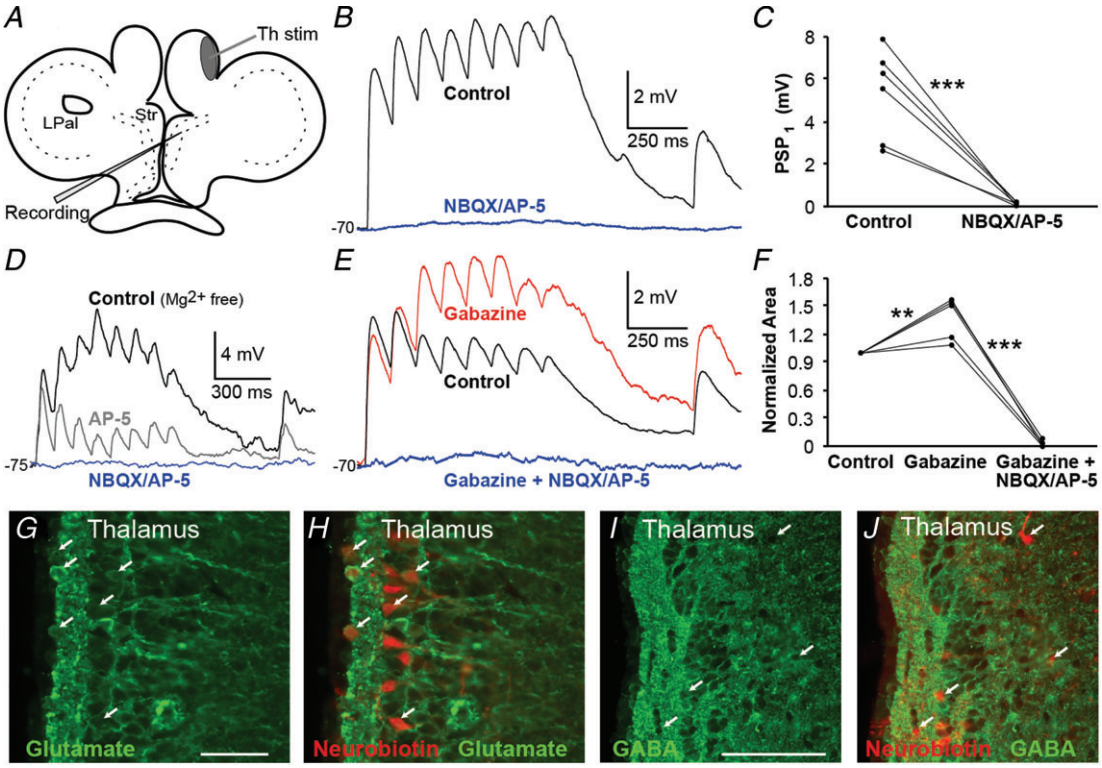

Figure 5. Thalamostriatal synaptic responses are glutamatergic
A, schematic drawing indicating stimulation area of Th fibres in the most lateral region of the medial pallium. *B*, striatal postsynaptic potentials (PSPs) in regular aCSF in response to stimulation of Th fibres (black trace) and application of NBQX (40 μM) and AP-5 (50 μM), that completely removed all responses (blue trace), quantified by comparing the amplitude of the first PSP before and after drug application (*C*). *D*, NMDA and AMPA receptors were investigated in Mg^{2+}-free aCSF by current-clamp recordings of striatal PSPs in response to stimulation of Th fibres (black trace), and after sequential application of AP-5 (grey trace) and both AP-5 and NBQX (blue trace) at about −75 mV. *E*, application of gabazine (20 μM, red trace) increased responses in recorded neurons (rest V_m −70 mV), indicative of oligosynaptic inhibition. Responses were completely removed by further application of NBQX and AP-5 (blue trace). *F*, quantification of the effect of drugs in (*E*). *G*, glutamate immunostaining (green) of the Th showed that the cell layer is packed with glutamatergic neurons. *H*, retrogradely labelled neurons (red) from the striatum are glutamatergic as indicated by the arrows and the co-staining. *I*, immunostaining for GABA (green) in the Th. *J*, retrogradely labelled neurons (red) were GABA-immunonegative as there was no co-staining with GABA. Scale bars, 50 μm in *G*; 100 μm in *I*. $^{**}P < 0.01$, $^{***}P < 0.001$, two-tailed paired *t* tests. LPal, lateral pallium; Str, striatum; Th, thalamus.

that were clearly depressing throughout the 8 pulses (Fig. 6*A*; $n = 16$, black trace). Synaptic responses from vLPal (Fig. 6*A*; $n = 10$, grey trace) were also depressing. The activity-dependent short-term synaptic facilitation of responses from LPal reached a maximum at the third pulse (ratio 1.58 ± 0.34), but responses were still facilitatory at the fourth pulse (ratio 1.28 ± 0.35). The synaptic dynamics of responses from the LPal were significantly different from the Th and vLPal for the first 300 ms after the first response; pulse 3 (Th 0.49 ± 0.08; vLPal 0.45 ± 0.12; $P < 0.01$) and pulse 4 (Th 0.45 ± 0.08; vLPal 0.25 ± 0.04; $P < 0.05$). In a comparison of responses of IRNs *versus* non-IRNs to Th and LPal stimulations, we did not discover any significant differences in the paired-pulse responses (Th PPRs: IRN 0.51 ± 0.08, non-IRN 0.60 ± 0.13, $P = 0.55$; LPal PPRs: IRN 1.46 ± 0.1, non-IRN 1.36 ± 0.18, $P = 0.77$).

To investigate if the different synapses had recovered 600 ms after the pulse train, a RTR (see Planert *et al.* 2010) was evoked and compared with the first PSP (last response in Fig. 6*A* and *D*). The test response recovered back to baseline during LPal stimulation (ratio 0.99 ± 0.16; Fig. 6*C*; n.s.), whereas the thalamostriatal test response was significantly depressed compared with baseline (ratio 0.55 ± 0.06; Fig. 6*C*; $P < 0.001$). Recovery responses from vLPal were also depressed (ratio 0.53 ± 0.04; Fig. 6*C*; $P < 0.001$). The differences in activity-dependent synaptic plasticity were also obtained when the same postsynaptic neuron was recorded in response to both LPal and Th extracellular stimulation. The PPRs were facilitatory and the test response recovered from stimulations of the LPal, while they were depressed for both Th and vLPal responses (example shown in Fig. 6*D*). This also shows that both LPal and Th inputs are capable of converging upon the same striatal neuron. Synaptic responses from LPal often summated over a longer time period, effectively integrating incoming input and driving the cell towards threshold rather than reaching a plateau at subthreshold levels as did responses to Th input (Fig. 6*C*; $n = 10/17$).

The results from the PPRs and RTRs both suggest a difference in presynaptic properties from the LPal and Th to striatum. The PPF and full recovery of responses

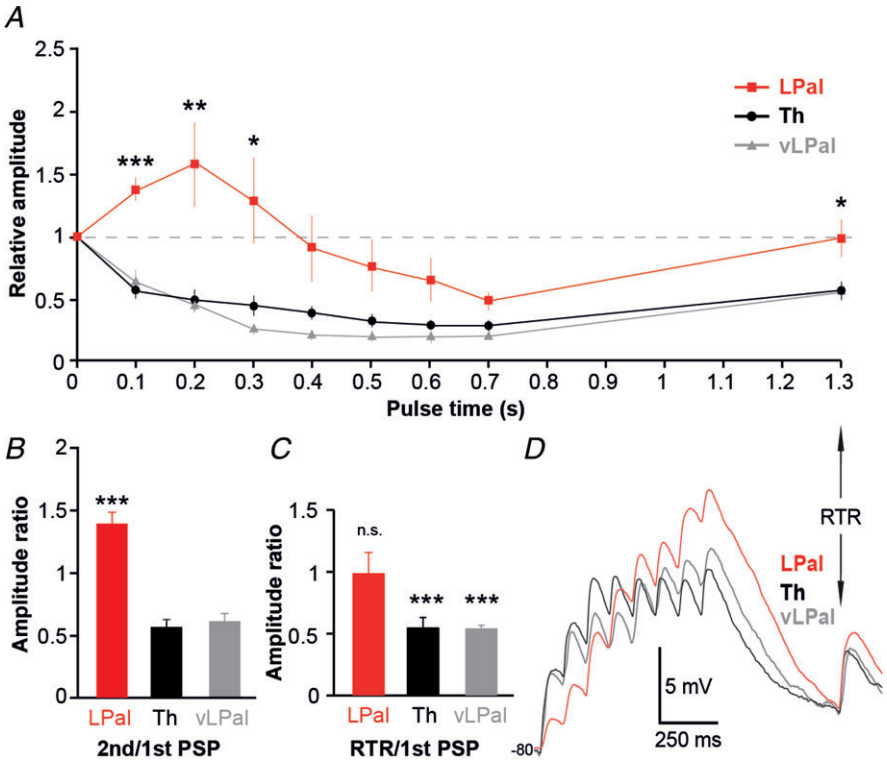

Figure 6. Lateral palliostriatal and thalamostriatal synapses have different dynamics
A, normalized postsynaptic responses to stimulations in lateral pallium (LPal; red squares), ventrolateral pallium (vLPal; grey triangles) and thalamus (Th; black circles) including the normalized recovery test response (RTR) 600 ms after the 8th pulse in the stimulus train. *B*, comparison of the paired-pulse ratio of the second postsynaptic potential (PSP) to the first PSP in response to stimulations of fibres from the Th, LPal and vLPal (Th PPD 0.56 ± 0.07; vLPal PPD 0.61 ± 0.12; $P < 0.001$ compared with LPal). *C*, comparisons of the RTR of LPal, vLPal and Th stimulation. *D*, postsynaptic response patterns in the same neuron to LPal (red), vLPal (grey) and Th (black) stimulations, baseline potential at −80 mV. $^*P < 0.05$, $^{**}P < 0.01$, $^{***}P < 0.001$, two-tailed paired *t* tests.

from LPal are both indicative of a low presynaptic release probability, whereas the PPD and depressed recovery of Th and vLPal responses suggest high presynaptic release probabilities. To investigate the release probability in further detail, we altered the external calcium concentration (Fig. 7) of the aCSF as there is a direct relationship between the probability of release and presynaptic calcium levels. By lowering the Ca^{2+} concentration from 2 mM to 0.5 mM, lateral palliostriatal PPF was increased from a ratio of 1.07 ± 0.12 to 1.50 ± 0.15 ($P < 0.05$, $n = 5$; Fig. 7*A* and *B*). An increase of the Ca^{2+} concentration to 4 mM did not significantly change the paired-pulse ratio, but there was a trend towards synaptic depression (0.81 ± 0.17, $P = 0.14$, $n = 5$; Fig. 7*A* and *B*). Similarly for thalamostriatal synaptic responses, lowering the Ca^{2+} concentration to 0.5 mM reduced the PPD from 0.59 ± 0.095 to 0.87 ± 0.10 ($P < 0.05$, $n = 5$; Fig. 7*C* and *D*). A few neurons even shifted from synaptic depression to facilitation and an increased summation of the entire response train was demonstrated (see example in Fig. 7*C*). Increasing the calcium concentration to 4 mM did not change the PPR ($P = 0.94$, $n = 5$; Fig. 7*D*). Together these results indicate that lateral palliostriatal synapses have low release probabilities compared with thalamostriatal synapses with higher release probabilities that, at least partly, underlie the difference in short-term synaptic responses. Similar differences are found in cortico- and thalamostriatal short-term synaptic plasticity in rodents (Ding *et al.* 2008, 2010; Ellender *et al.* 2011).

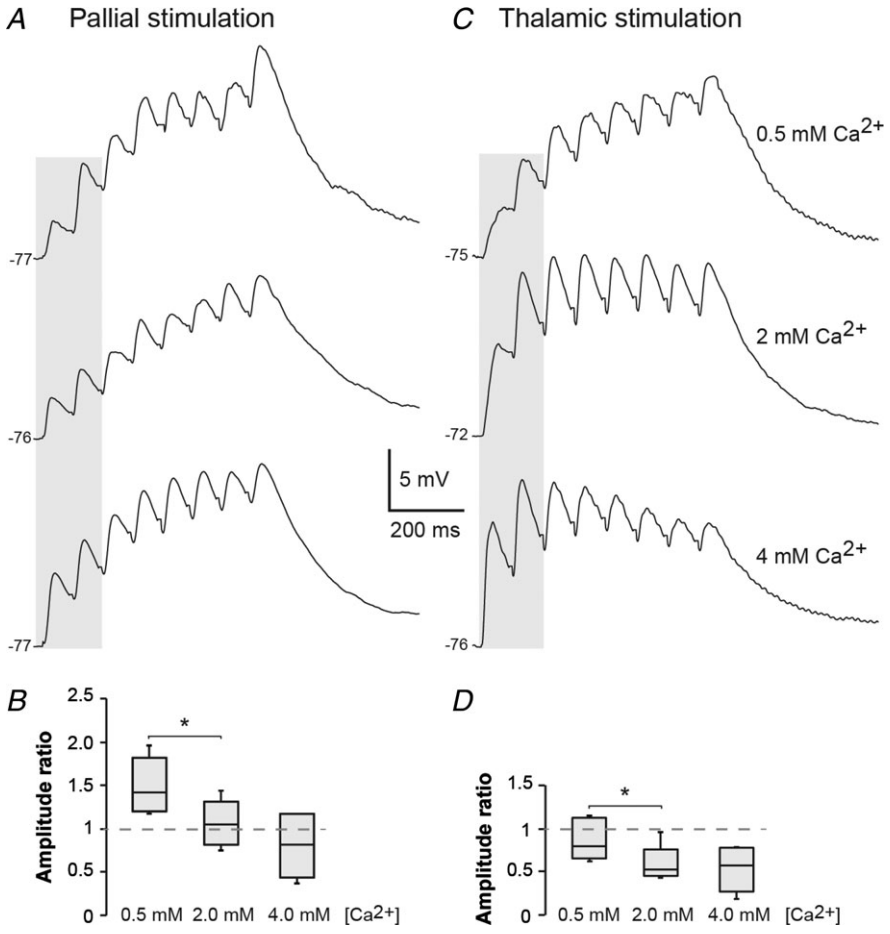

Figure 7. Altering extracellular calcium concentration changes striatal short-term synaptic plasticity from the LPal and Th

A, postsynaptic voltage responses to stimulation of the LPal in three different extracellular Ca^{2+} concentrations: 0.5 mM (top trace); 2 mM (middle trace); and 4 mM (bottom trace). *B,* box-plot of the paired-pulse ratio of the first two palliostriatal responses (grey shading in *A*) that was increased by lowering the Ca^{2+} concentration to 0.5 mM compared with the regular aCSF calcium concentration of 2 mM. *C,* voltage responses to stimulation of thalamostriatal fibres in the same conditions as in *A*. *D,* box-plot of the paired-pulse ratio of the first two thalamostriatal responses (shading in *C*) where the synaptic depression was decreased in 0.5 mM Ca^{2+} concentration. $^*P < 0.05$.

Intrastriatal stimulation evokes a mix of GABAergic and glutamatergic responses

We also applied the same type of train stimuli within the striatum, but in this case we would anticipate coactivation of the LPal, Th and modulatory input together with responses from the striatal microcircuit. The stimulation electrode was placed centrally or ventrally within the striatal cell band or just lateral to it (Fig. 8*A*). Synaptic responses were readily evoked (Fig. 8*B*, black trace) and application of NBQX and AP-5 significantly reduced, but did not abolish, the postsynaptic responses ($\text{control}_{\text{PSP1}}$ 2.70 ± 0.58 mV, $\text{NBQX/AP-5}_{\text{PSP1}}$ 0.69 ± 0.15 mV, $P < 0.05$, $n = 5$; Fig. 8*B* and *C*). An additional application of gabazine (Fig. 7*B*, grey trace) did, however, completely remove the response ($\text{gabazine/NBQX/AP-5}_{\text{PSP1}}$ 0.026 ± 0.03 mV, $P < 0.01$, $n = 5$; Fig. 8*B* and *C*). Thus, in contrast to stimulation of the LPal and Th input, the GABAergic striatal network was directly recruited by this stimulation.

Responses to intrastriatal stimulation were depressing (Fig. 8*B*, black trace), and result from a mix of excitatory and inhibitory synaptic responses. Because Th and LPal projections to the striatum are glutamatergic, the isolated GABAergic component after application of NBQX/AP-5 (Fig. 8*B* and *D*, blue traces) will most likely originate only from intrastriatal synaptic interactions. The paired-pulse ratio of intrastriatal GABAergic responses was 0.74 ± 0.07 (Fig. 8*E*; $n = 5$), measured from both rectifying and non-rectifying neurons. This response was significantly different from the LPal input (compare Figs 6*B* and 7*E*; $P < 0.01$), but not from that of the Th or the vLPal ($P > 0.05$). The RTR was also depressed compared with the baseline synaptic response (0.47 ± 0.11; Fig. 8*E*; $P < 0.01$). The results thus indicate that the intrastriatal GABAergic synaptic inhibition displays short-term synaptic depression and that the recovery of synapses is longer than 600 ms.

Discussion

The general aim of the present study was to identify the synaptic characteristics of the input from the Th and LPal to striatal neurons. The principal findings are that synaptic inputs to the striatum from the LPal and Th are excitatory and glutamatergic, act via both NMDA and AMPA receptors, and that these afferents have opposite synaptic dynamics. In addition, the excitatory input recruits activity-dependent oligosynaptic GABAergic inhibition within the intrastriatal network, which may be a result of feedforward inhibition mediated by GABAergic fast-spiking neurons or feedback inhibition by projection neurons previously described in the lamprey striatum (Ericsson *et al.* 2011). The synaptic properties share similar characteristics to those established in mammals, indicating

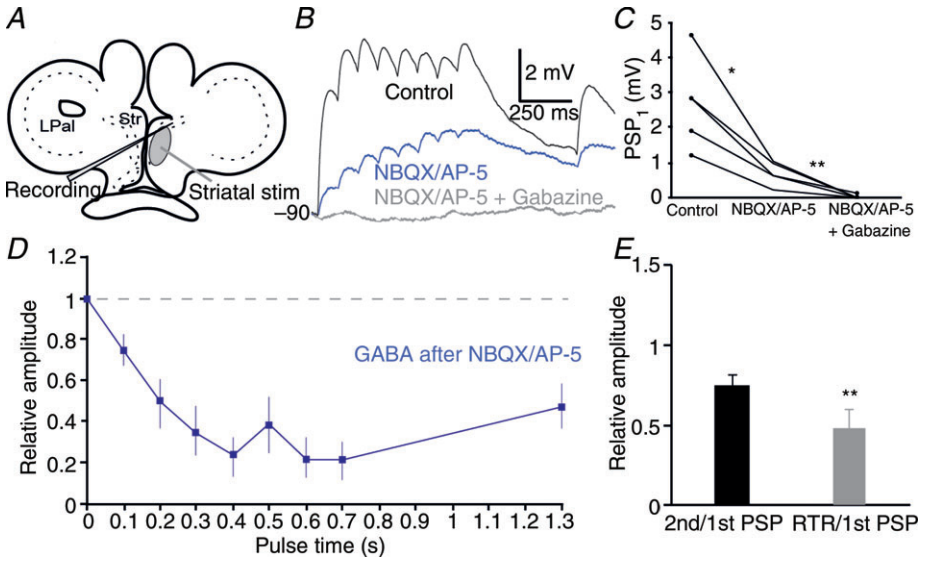

Figure 8. Intrastriatal stimulation evokes glutamatergic and GABAergic responses
A, schematic drawing indicating stimulation area in the striatum (Str). *B*, striatal postsynaptic potentials (PSPs; black trace) in response to intrastriatal stimulation and application of NBQX (40 μM) and AP-5 (50 μM) significantly reduces postsynaptic responses (blue trace), but they were only completely removed after additional application of gabazine (20 μM, grey trace). Neurons were held at hyperpolarized potentials where GABA is depolarizing, here at −90 mV. *C*, quantification of the synaptic effects of drugs was performed by comparing the amplitude of the first PSP in the pulse train. *D*, normalized postsynaptic depressing intrastriatal GABAergic responses, isolated after application of NBQX and AP-5. *E*, the paired-pulse ratio (black) and the recovery test ratio (RTR; grey) of GABAergic responses that are both depressed. $^*P < 0.05$, $^{**}P < 0.01$, two-tailed paired *t* tests. LPal, lateral pallium.

that the difference in short-term synaptic plasticity is conserved throughout vertebrate evolution.

The synaptic dynamics from the Th is different from that of the LPal

Stimulation of the Th fibres results in short-term synaptic depression, in contrast to the LPal responses that are facilitatory. This difference in synaptic properties is similar to that of rodents, where repeated Th input onto MSNs evokes marked synaptic depression (Ding *et al.* 2008, 2010; Ellender *et al.* 2011), whereas the corticostriatal connection is instead facilitatory over several pulses in a stimulation train (Smith *et al.* 2001; Ding *et al.* 2008, 2010; Ellender *et al.* 2011). However, varying the interstimulus intervals of the corticostriatal activation may sometimes also lead to synaptic depression in rodents (Smeal *et al.* 2007; Goubard *et al.* 2011). Thus, the functional difference between the main excitatory striatal afferents in rodents appears to be present already in lamprey.

Why do we have this conserved difference in synaptic properties between cortex/pallium and Th from lamprey to mammals? It would seem likely that it reflects a difference in the functional role of the two inputs. Possibly the Th input will provide fast direct access to the striatum (e.g. from sensory input), whereas the input channelled via the cortex/pallium will require more time but be further processed and subsequently provide a more maintained signal to the striatum.

The difference in short-term synaptic plasticity in rodents is due to presynaptic properties (Ding *et al.* 2008), which appears to be the case also between lamprey thalamostriatal and lateral palliostriatal fibres onto striatal neurons. As shown in the Results, the same neuron will receive facilitatory synapses from the LPal and depressing synapses from the Th, supporting a presynaptic origin. The PPD and RTR typical of Th responses are both indicative of a high presynaptic release probability and possible depletion of vesicles (Thomson, 2000), leading to progressively less release of transmitters during a prolonged stimulation. We also showed this directly by lowering the external calcium concentration that reduces synaptic depression, consistent with a high release probability at physiological calcium levels. The high release probability is also consistent with the response plateau seen during the stimulus train. Conversely, the PPF and complete recovery of responses from stimulation of the LPal suggest a low presynaptic release probability (Thomson, 2000). This was shown directly by the increased PPF in low extracellular calcium levels. The low release probability may also explain the more efficient temporal summation, as consecutive pulses lead to an increased presynaptic calcium influx and transmitter release. However, although Th and LPal input only produced monosynaptic glutamatergic responses, the activity-dependent recruitment of GABA at pulse 3 or later affects the summation or responses (Figs 4 and 5). Thus, the synaptic dynamics during prolonged activity is likely a combination of the presynaptic properties, postsynaptic depolarization and oligosynaptic inhibition.

The synaptic effects of stimulation of the vLPal are depressing. Very few cells were retrogradely labelled from the striatum in this area (Fig. 1*A*), which would suggest that fibres of uncertain origin were activated. A second Th projection has previously been described (Polenova & Vesselkin, 1993; Northcutt & Wicht, 1997) with fibres in the vLPal. There is thus the possibility that stimulation here activates Th afferents onto striatal dendrites that are abundant in this area (Ericsson *et al.* 2011). If so, these results may represent the activation of a second thalamostriatal projection that is depressing. These Th fibres were, however, few in our anatomical studies, confirming earlier results that the main thalamostriatal projection goes via the lateral region of the medial pallium (Polenova & Vesselkin, 1993).

The glutamatergic and oligosynaptic GABAergic striatal input

Although it has been shown that striatal neurons receive spontaneous barrages of glutamatergic and GABAergic input (Ericsson *et al.* 2007, 2011), very little was known about the origin of these afferents and their synaptic characteristics. The preservation of Th fibres in the separate and well-defined lateral region of the medial pallium in a transverse brain slice preparation (Fig. 2*A*) made it possible to specifically activate this striatal input. A few neurons in the caudal medial pallium were also found to project to the striatum, but they were located on the opposite side to that of the Th bundle (see also Pombal *et al.* 1997*a*) and are GABAergic (Robertson *et al.* 2007). No glutamatergic cells are located in the medial pallium (Villar-Cerviño *et al.* 2011). Taken together, these findings support our assumption that only Th glutamatergic fibres were activated in this region.

The fact that the Th and LPal inputs activate both NMDA and AMPA receptors is important as NMDA receptor activation is critical for induction of different long-term changes in synaptic transmission at many synapses, including mammalian corticostriatal synapses (Calabresi *et al.* 1992; Partridge *et al.* 2000). As has been shown in mammals, the NMDA/AMPA ratio was higher for the palliostriatal input than for the thalamostriatal input (Ding *et al.* 2008), which also applies to the lamprey but at a slightly lower level. The higher abundance of NMDA receptors at palliostriatal synapses probably acts in concert with the facilitatory nature of these synapses, potentially as important mechanisms for the transition

from a resting hyperpolarized potential towards threshold, as has been indicated previously (Surmeier *et al.* 2007; Ding *et al.* 2008).

The afferent excitation also elicited di- or oligosynaptic inhibition, most likely originating in the striatum as direct striatal activation always recruits the densely packed striatal GABAergic microcircuit (Pombal *et al.* 1997*a*; Menard *et al.* 2007; Robertson *et al.* 2007). It is not yet clear if this inhibition is mediated via two (disynaptic) or more (oligosynaptic) synapses. The inhibition reduces the temporal summation of EPSPs, and thereby it affects and partly controls the striatal integration of incoming excitation. In the mammalian system this is achieved via GABAergic interneurons and axon collaterals of MSNs (Buchwald *et al.* 1973; Koos & Tepper, 1999; Suzuki *et al.* 2001; Tepper *et al.* 2004), where they provide the striatum with feedforward and feedback mechanisms (Mallet *et al.* 2005; Gittis *et al.* 2010; Klaus *et al.* 2011). Striatal stimulation evoked a GABAergic depressing signal in both rectifying neurons expressing Kir-channels and non-rectifying neurons, suggesting both neuronal types are affected. It is, however, unknown if this occurs via fast-spiking or other GABAergic interneurons or via axon collaterals of the output neurons. As an indication, however, two striatal neurons were recorded interacting via a depressing synapse activated by a stimulus train (unpublished data, JE). It is thus possible that similar connections of inter- and/or output neurons underlie the oligosynaptic inhibition.

Ericsson *et al.* (2011) reported an even distribution of rectifying ($n = 30$) and non-rectifying ($n = 32$) neurons, separated with respect to a rectification index of 0.5. This boundary may be too conservative, and in identified avian projection neurons, the dividing line is set to a rectification index of 0.75 (Farries *et al.* 2005). With the border set at 0.75, 80% of the striatal neurons in Ericsson *et al.* (2011; see their fig. 2B) would be classified as rectifying neurons, which would seem reasonable. We recently also showed that striatonigral projection neurons are IRNs that selectively express substance P and dopamine D1 receptors (Ericsson, 2012; Stephenson-Jones *et al.* 2012).

Functional implications

The LPal and Th signals provide different types of information to the striatum, which may be reflected in the difference in dynamic properties. The LPal receives strong afferent input from the olfactory bulbs (Northcutt & Puzdrowski, 1988; Derjean *et al.* 2010), septum, preoptic area, medial pallium and Th (Northcutt & Wicht, 1997). The signals to the striatum from the LPal may thus be related to sensorimotor integration arising from olfactory and other sensory modalities.

Although the role of the LPal area in basic motor function is not known, recent experiments show that electrical microstimulation of specific regions of the LPal evokes movements of the eye, mouth and head as well as locomotion, depending on the stimulation parameters (Ocaña *et al.* 2011). These effects may be partially exerted via the lateral palliostriatal projection, and movements can also be elicited by direct striatal stimulation (Menard & Grillner, 2008; Ocaña *et al.* 2011). The LPal thus appears to process information closely related to motor and somatosensory signalling. The facilitatory properties of lateral palliostriatal synaptic responses may reflect an integrative function specific to this input, and the effective temporal summation may drive cells to spike during persistent activity over longer time periods. This may suggest that synchronized inputs will have a larger effect and potentially filter out small synaptic events that are uncorrelated.

The lamprey Th receives a different input, including direct retinal and tectal input (Vesselkin *et al.* 1980) and input from the olfactory bulbs, the nucleus of the posterior commissure nucleus and the torus semicircularis (Polenova & Vesselkin, 1993; Northcutt & Wicht, 1997). Studies in other vertebrates have shown that the Th and its projection to the striatum from the intralaminar nucleus may be involved in the shift of attention and specifically signals upon salient information such as prey (Ewert *et al.* 1999; Matsumoto *et al.* 2001; Smith *et al.* 2004). In mammals (Ding *et al.* 2008, 2010) as well as in lamprey, the Th input is depressing. Instead of effective temporal summation, these responses quickly reach a subthreshold plateau due to strong synaptic depression. This indicates that striatal neurons may respond most strongly to sudden, precisely timed, coincident Th inputs, whereas persistent activity will be depressed already at the second response.

In summary, the Th and LPal provide the striatum with direct excitatory glutamatergic input of opposite synaptic dynamics that is conserved from lamprey to man.

References

Barral J, Galarraga E, Tapia D, Flores-Barrera E, Reyes A & Bargas J (2010). Dopaminergic modulation of spiny neurons in the turtle striatum. *Cell Mol Neurobiol* **30**, 743–750.

Brodin L, Hokfelt T, Grillner S & Panula P (1990*a*). Distribution of histaminergic neurons in the brain of the lamprey Lampetra fluviatilis as revealed by histamine-immunohistochemistry. *J Comp Neurol* **292**, 435–442.

Brodin L, Theordorsson E, Christenson J, Cullheim S, Hökfelt T, Brown J, Buchan A, Panula P, Verhofstad A & Goldstein M (1990*b*). Neurotensin-like peptides in the CNS of lampreys: chromatographic characterisation and immunohistochemical localisation with reference to aminergic markers. *Eur J Neurosci* **2**, 1095–1109.

Buchwald NA, Price DD, Vernon L & Hull CD (1973). Caudate intracellular response to thalamic and cortical inputs. *Exp Neurol* **38**, 311–323.

Calabresi P, Pisani A, Mercuri NB & Bernardi G (1992). Long-term potentiation in the striatum is unmasked by removing the voltage-dependent magnesium block of NMDA receptor channels. *Eur J Neurosci* **4**, 929–935.

Derjean D, Moussaddy A, Atallah E, St-Pierre M, Auclair F, Chang S, Ren X, Zielinski B & Dubuc R (2010). A novel neural substrate for the transformation of olfactory inputs into motor output. *PLoS Biol* **8**, e1000567.

Ding J, Peterson JD & Surmeier DJ (2008). Corticostriatal and thalamostriatal synapses have distinctive properties. *J Neurosci* **28**, 6483–6492.

Ding JB, Guzman JN, Peterson JD, Goldberg JA & Surmeier DJ (2010). Thalamic gating of corticostriatal signaling by cholinergic interneurons. *Neuron* **67**, 294–307.

Ellender TJ, Huerta-Ocampo I, Deisseroth K, Capogna M & Bolam JP (2011). Differential modulation of excitatory and inhibitory striatal synaptic transmission by histamine. *J Neurosci* **31**, 15340–15351.

Ericsson J, Robertson B & Wikstrom MA (2007). A lamprey striatal brain slice preparation for patch-clamp recordings. *J Neurosci Meth* **165**, 251–256.

Ericsson J, Silberberg G, Robertson B, Wikstrom MA & Grillner S (2011). Striatal cellular properties conserved from lampreys to mammals. *J Physiol* **589**, 2979–2992.

Ericsson (2012). Cellular and synaptic properties in the lamprey striatum. Diss., Karolinska Institutet.

Ewert JP, Buxbaum-Conradi H, Glagow M, Röttgen A, Schürg-Pfeiffer E & Schwippert WW (1999). Forebrain and midbrain structures involved in prey-catching behaviour of toads: stimulus-response mediating circuits and their modulating loops. *Eur J Morphol* **37**, 172–176.

Farries MA, Meitzen J & Perkel DJ (2005). Electrophysiological properties of neurons in the basal ganglia of the domestic chick: conservation and divergence in the evolution of the avian basal ganglia. *J Neurophysiol* **94**, 454–467.

Farries MA & Perkel DJ (2000). Electrophysiological properties of avian basal ganglia neurons recorded in vitro. *J Neurophysiol* **84**, 2502–2513.

Gittis AH, Nelson AB, Thwin MT, Palop JJ & Kreitzer AC (2010). Distinct roles of GABAergic interneurons in the regulation of striatal output pathways. *J Neurosci* **30**, 2223–2234.

Goubard V, Fino E & Venance L (2011). Contribution of astrocytic glutamate and GABA uptake to corticostriatal information processing. *J Physiol* **589**, 2301–2319.

Graybiel AM (2005). The basal ganglia: learning new tricks and loving it. *Curr Opin Neurobiol* **15**, 638–644.

Grillner S, Hellgren J, Menard A, Saitoh K & Wikstrom MA (2005). Mechanisms for selection of basic motor programs–roles for the striatum and pallidum. *Trends Neurosci* **28**, 364–370.

Institute of Laboratory Animal Research, Commission on Life Sciences, National Research Council. Guide for the Care and Use of Laboratory Animals. Washington, DC: The National Academies Press, 1996.

Jimenez AJ, Mancera JM, Pombal MA, Perez-Figares JM & Fernandez-Llebrez P (1996). Distribution of galanin-like immunoreactive elements in the brain of the adult lamprey Lampetra fluviatilis. *J Comp Neurol* **368**, 185–197.

Kawaguchi Y, Wilson CJ & Emson PC (1989). Intracellular recording of identified neostriatal patch and matrix spiny cells in a slice preparation preserving cortical inputs. *J Neurophysiol* **62**, 1052–1068.

Klaus A, Planert H, Hjorth JJ, Berke JD, Silberberg G & Kotaleski JH (2011). Striatal fast-spiking interneurons: from firing patterns to postsynaptic impact. *Front Syst Neurosci* **5**, 57.

Koos T & Tepper JM (1999). Inhibitory control of neostriatal projection neurons by GABAergic interneurons. *Nat Neurosci* **2**, 467–472.

Kumar S & Hedges S (1998). A molecular timescale for vertebrate evolution. *Nature* **392**, 917–920.

Mallet N, Le Moine C, Charpier S & Gonon F (2005). Feedforward inhibition of projection neurons by fast-spiking GABA interneurons in the rat striatum in vivo. *J Neurosci* **25**, 3857–3869.

Marín O, Smeets W & González A (1998). Evolution of the basal ganglia in tetrapods: a new perspective based on recent studies in amphibians. *Trends Neurosci* **21**, 487–494.

Matsumoto N, Minamimoto T, Graybiel AM & Kimura M (2001). Neurons in the thalamic CM-Pf complex supply striatal neurons with information about behaviorally significant sensory events. *J Neurophysiol* **85**, 960–976.

Matute C & Streit P (1986). Monoclonal antibodies demonstrating GABA-like immunoreactivity. *Histochemistry* **86**, 147–157.

Menard A, Auclair F, Bourcier-Lucas C, Grillner S & Dubuc R (2007). Descending GABAergic projections to the mesencephalic locomotor region in the lamprey Petromyzon marinus. *J Comp Neurol* **501**, 260–273.

Menard A & Grillner S (2008). Diencephalic locomotor region in the lamprey–afferents and efferent control. *J Neurophysiol* **100**, 1343–1353.

Northcutt RG & Puzdrowski RL (1988). Projections of the olfactory bulb and nervus terminalis in the silver lamprey. *Brain Behav Evol* **32**, 96–107.

Northcutt RG & Wicht H (1997). Afferent and efferent connections of the lateral and medial pallia of the silver lamprey. *Brain Behav Evol* **49**, 1–19.

Ocaña FM, Saitoh K, Rodraguez F, Robertson B & Grillner S (2011). Is there a motor pallium in the lamprey. 8th IBRO World Congress of Neuroscience, Florence, B263.

Partridge JG, Tang KC & Lovinger DM (2000). Regional and postnatal heterogeneity of activity-dependent long-term changes in synaptic efficacy in the dorsal striatum. *J Neurophysiol* **84**, 1422–1429.

Planert H, Szydlowski SN, Hjorth JJ, Grillner S, Silberberg G (2010) Dynamics of synaptic transmission between fast-spiking interneurons and striatal projection neurons of the direct and indirect pathways. *J Neurosci* **30,**3499–3507.

Polenova OA & Vesselkin NP (1993). Olfactory and nonolfactory projections in the river lamprey (*Lampetra fluviatilis*) telencephalon. *J Hirnforsch* **34**, 261–279.

Pombal MA, El Manira A & Grillner S (1997*a*). Organization of the lamprey striatum – transmitters and projections. *Brain Res* **766**, 249–254.

Pombal MA, El Manira A & Grillner S (1997*b*). Afferents of the lamprey striatum with special reference to the dopaminergic system: a combined tracing and immunohistochemical study. *J Comp Neurol* **386**, 71–91.

Reiner A, Medina L & Veenman C (1998). Structural and functional evolution of the basal ganglia in vertebrates. *Brain Res Brain Res Rev* **28**, 235–285.

Robertson B, Auclair F, Menard A, Grillner S & Dubuc R (2007). GABA distribution in lamprey is phylogenetically conserved. *J Comp Neurol* **503**, 47–63.

Robertson B, Huerta-Ocampo I, Ericsson J, Stephenson-Jones M, Pérez-Fernández J, Bolam P, Diaz-Heijtz R & Grillner S (2012). The dopamine D2 receptor gene in lamprey, its expression in the striatum and cellular effects of D2 receptor activation. *PLoS ONE* **7**(4), e35642.

Robertson B, Saitoh K, Menard A & Grillner S (2006). Afferents of the lamprey optic tectum with special reference to the GABA input: combined tracing and immunohistochemical study. *J Comp Neurol* **499**, 106–119.

Smeal RM, Gaspar RC, Keefe KA & Wilcox KS (2007). A rat brain slice preparation for characterizing both thalamostriatal and corticostriatal afferents. *J Neurosci Meth* **159**, 224–235.

Smeets WJ, Marin O & Gonzalez A (2000). Evolution of the basal ganglia: new perspectives through a comparative approach. *J Anat* **196**, 501–517.

Smith R, Musleh W, Akopian G, Buckwalter G & Walsh JP (2001). Regional differences in the expression of corticostriatal synaptic plasticity. *Neuroscience* **106**, 95–101.

Smith Y, Raju DV, Pare JF & Sidibe M (2004). The thalamostriatal system: a highly specific network of the basal ganglia circuitry. *Trends Neurosci* **27**, 520–527.

Stephenson-Jones M, Ericsson J, Robertson B & Grillner S (2012). Evolution of the basal ganglia; dual output pathways conserved throughout vertebrate phylogeny. *J Comp Neurol* **520**, 2957–2973.

Stephenson-Jones M, Samuelsson E, Ericsson J, Robertson B & Grillner S (2011). Evolutionary conservation of the basal ganglia as a common vertebrate mechanism for action selection. *Curr Biol* **21**, 1081–1091.

Surmeier DJ, Ding J, Day M, Wang Z & Shen W (2007). D1 and D2 dopamine-receptor modulation of striatal glutamatergic signaling in striatal medium spiny neurons. *Trends Neurosci* **30**, 228–235.

Suzuki T, Miura M, Nishimura K & Aosaki T (2001). Dopamine-dependent synaptic plasticity in the striatal cholinergic interneurons. *J Neurosci* **21**, 6492–6501.

Tepper JM, Koos T & Wilson CJ (2004). GABAergic microcircuits in the neostriatum. *Trends Neurosci* **27**, 662–669.

Thomson AM (2000). Facilitation, augmentation and potentiation at central synapses. *Trends Neurosci* **23**, 305–312.

Vesselkin NP, Ermakova TV, Reperant J, Kosareva AA & Kenigfest NB (1980). The retinofugal and retinopetal systems in Lampetra fluviatilis. An experimental study using radioautographic and HRP methods. *Brain Res* **195**, 453–460.

Villar-Cerviño V, Barreiro-Iglesias A, Mazan S, Rodicio MC, Anadón R (2011). Glutamatergic neuronal populations in the forebrain of the sea lamprey, Petromyzon marinus: an *in situ* hybridisation and immunocytochemical study. *J Comp Neurol* **519**, 1712–1735.

Author contributions

J.E. conducted the patch-clamp experiments and primary data analysis, and developed the experimental design together with G.S., M.S.J. and S.G. M.S.J. performed the anatomical and immunohistochemical experiments and analysis and A.K. assisted J.E. with some of the patch-clamp experiments. All authors took part in the evaluation of the experimental data, and J.E. wrote the manuscript in interaction with all authors. All authors approved the final version.

Acknowledgements

This work was supported by the Swedish Research Council, HEALTH-F2–2008-201716 Select-and-Act, ICT-STREP 216100-LAMPETRA, and the Karolinska Institute. We are grateful to Drs Peter Wallén and Abdel El Manira for valuable comments on the manuscript.